Antisite disorder and bond valence compensation in Li_2FePO_4F cathode for Li-Ion batteries

Antisite disorder and bond valence compensation in Li_2FePO_4F cathode for Li-Ion batteries

Olesia M. Karakulina, Nellie R. Khasanova, Oleg A. Drozhzhin, Alexander A. Tsirlin, Joke Hadermann, Evgeny V. Antipov, Artem M. Abakumov.

Publisher's version: O. M. Karakulina, et al., Antisite Disorder and Bond Valence Compensation in Li_2FePO_4F Cathode for Li-Ion Batteries, Chemistry of Materials 2016 28 (21), 7578-7581

DOI: 10.1021/acs.chemmater.6b03746

http://dx.doi.org/10.1021/acs.chemmater.6b03746

Antisite disorder and bond valence compensation in Li_2FePO_4F cathode for Li-ion batteries.

Olesia M. Karakulina[†], Nellie R. Khasanova[‡], Oleg A. Drozhzhin[‡,§], Alexander A. Tsirlin[∥,⊥], Joke Hadermann[†], Evgeny V. Antipov[‡] and Artem M. Abakumov[§,†,*]

[†]EMAT, University of Antwerp, Groenenborgerlaan 171, B-2020, Antwerp, Belgium

[‡]Department of Chemistry, Lomonosov Moscow State University, 119991 Moscow, Russia

[§]Skoltech Center for Electrochemical Energy Storage, Skolkovo Institute of Science and Technology, Nobel str. 3, 143026 Moscow, Russian Federation

[∥]Experimental Physics VI, Center for Electronic Correlations and Magnetism, University of Augsburg, 86159 Augsburg, Germany

[⊥]National Institute of Chemical Physics and Biophysics, Akadeemia tee 23, 12618 Tallinn, Estonia

KEYWORDS Li-ion battery, polyanion cathode, fluorophosphate, antisite disorder

ABSTRACT: We report on a remarkable Li/Fe antisite disorder upon electrochemical cycling of the Li_2FePO_4F cathode for Li-ion batteries. As reflected by electron diffraction tomography structure analysis, up to 30-40% of Fe is located in the Li positions after 10 charge-discharge cycles at room temperature and at 75 °C. This massive antisite disorder is attributed to the peculiarities of the three-dimensional framework structure of Li_2FePO_4F: the presence of oxygen atoms linked exclusively to Li and P atoms ("dangling" P-O bonds) and oxygen atoms at the common edges of the edge-sharing FeO_4F_2 octahedra. Li deintercalation results in underbonding of the O atoms at the "dangling" P-O bonds that is compensated by a migration of the Fe^{3+} cation to the Li sites. At the same time, the Li cations migrating to the Fe sites relieve overbonding of the O atoms at the common edge of the FeO_4F_2 octahedra. Olivine-structured $LiFePO_4$ having no such structural features, does not demonstrate antisite disorder being cycled even at 100 °C. Bond valence compensation for the oxygen atoms in the "dangling" bonds of polyanion groups is suggested to be a triggering factor for antisite disorder in polyanion cathode materials.

Transition-metal (TM) cation migration has always been considered detrimental for the performance of cathode (positive electrode) materials for metal-ion batteries. In layered oxides based on the rock-salt structure, the TM cations can migrate from their original octahedral sites toward the empty octahedra in the Li layers upon charge and return upon discharge, as observed in the Li-rich $Li_2Ru_{1-y}Ti_yO_3$ phases.[1] This process is only partially reversible and leaves a fraction of the TM cations trapped at the tetrahedral interstices of the close-packed oxygen array, resulting in a gradual voltage fade.[1,2] Migration of the TM cations to the Li positions can also induce irreversible phase transformations (e.g. layered $Li_{0.5}MO_2$ to spinel LiM_2O_4) and negatively affect the electrode kinetics due to blocking the Li diffusion pathway.[3-7] Although some cation-disordered materials can demonstrate facile Li diffusion due to the presence of percolation diffusion channels,[8] the perfect ordering of the TM and alkali cations is generally regarded beneficial for the electrochemical performance.[9,10]

Compared to the layered oxides much less is known on the TM-alkali metal disorder in the polyanion cathodes. Olivine-structured $LiFePO_4$ as the commercially deployed material is, perhaps, the most scrutinized in this aspect. Owing to the similar ionic radii of the Li^+ and Fe^{2+} cations in the octahedral oxygen environment (0.76Å and 0.78Å, respectively),[11] antisite Li/Fe disorder is possible corresponding to the Kröger–Vink equation:

$$Li_{Li}^{\times} + Fe_{Fe}^{\times} \rightarrow Li_{Fe}^{'} + Fe_{Li}^{\bullet} \qquad (1)$$

Among other intrinsic defects, the Li-Fe antisite defect pairs are of the lowest energy,[12] and these defects are indeed present in pristine $LiFePO_4$ with concentration up to 10% depending on preparation conditions.[13,14] The antisite defects in $LiFePO_4$ deteriorate the Li mobility slowing down the Li diffusion in the [010] channels of the olivine structure.[15] However, in contrast to the layered oxides, the antisite defects in $LiFePO_4$ are not induced by electrochemical cycling, although increasing Li-Co disorder associated with a progressive capacity fade has been reported for the $LiCoPO_4$ olivine-structured cathode.[16]

Taking into account the importance of cation disorder for the electrochemical properties of cathode materials, we monitored the crystal structure of another potential polyanion fluoride-phosphate cathode material Li_2FePO_4F.[17,18] This material belongs to a so-called 3-dimensional A_2MPO_4F polymorphic structure and can be prepared by electrochemical exchange of Li for Na in $LiNaFePO_4F$.[17] Surprisingly, already after ten charge/discharge cycles in the Li-cell we observed massive Li/Fe disorder in the resulting Li_2FePO_4F material. In the following, we report on the crystal structures of thus prepared compounds, compare the anitsite defect formation with its $LiFePO_4$ counterpart, and speculate on the possible driving force for such pronounced antisite disorder.

$LiNaFePO_4F$ was prepared by a solid-state reaction of $LiFePO_4$ with NaF at 670°C, and then Na was exchanged electrochemically with Li by cycling the material in the 2.6–4.0V potential range *vs* Li/Li^+ in a $LiBF_4$/TMS electrolyte using metallic Li as anode (see details in Supporting information). The cation exchange was per-

formed at 75 °C in order to speed up cation diffusion and obtain a Na-free product. Indeed, EDX analysis in a transmission electron microscope revealed the absence of the Na-K signal (Fig. S3 of Supporting information) confirming that Na is completely replaced by Li and Li_2FePO_4F is obtained (this sample is denoted further as Li_2FePO_4F-75).

The crystal structure of Li_2FePO_4F was analyzed with electron diffraction tomography. In this technique, the reciprocal space of a submicron single crystal in a powder sample is scanned by collecting reciprocal lattice sections with a small angular step (1° in our case). The integrated quasi-kinematic electron diffraction intensities are combined into a 3D dataset, which can be used for structure refinement. We have recently demonstrated the applicability of this method to such cathode materials as $Li_{1-x}Fe_{0.5}Mn_{0.5}PO_4$ and $(Li,K)_{1-x}VPO_4F$.[19,20] Surprisingly, the structure refinement and difference Fourier maps of the discharged Li_2FePO_4F-75 structure reveal overestimated scattering density in the Li positions (particularly, in the position Li2) and substantial deficiency of the scattering density at the Fe positions (see a difference Fourier map in Fig. 1a and details of the crystallographic analysis in Supporting information, Tables S1-S3). This unequivocally suggests the presence of Li/Fe antisite disorder. Mixing of the Li and Fe cations at the 3 Li and 2 Fe sites and the refinement of the occupancy factors significantly improves the agreement between the observed and calculated structure factors (Fig. S5), decreases the reliability factor from R_F = 0.295 to R_F = 0.219, and eliminates the positive and negative maxima on the difference Fourier map (Fig. 1b). In the resulting structure, the Fe1 and Fe2 positions contain ~30% and 40% Li, respectively, whereas the largest fraction of Fe resides in the Li2 position (36%) and the Li1 and Li3 positions contain only 10-12% of Fe (Table S2).

As such a massive antisite disorder is not common in polyanion cathode materials, it is interesting to understand what causes this substantial Li and Fe mixing. The elevated temperature of the electrochemical cation exchange would be a plausible driving force for the cation disorder. Thus, we performed the cation exchange using the same procedure, but at room temperature and refined the crystal structure of the obtained Li_2FePO_4F-RT compound.

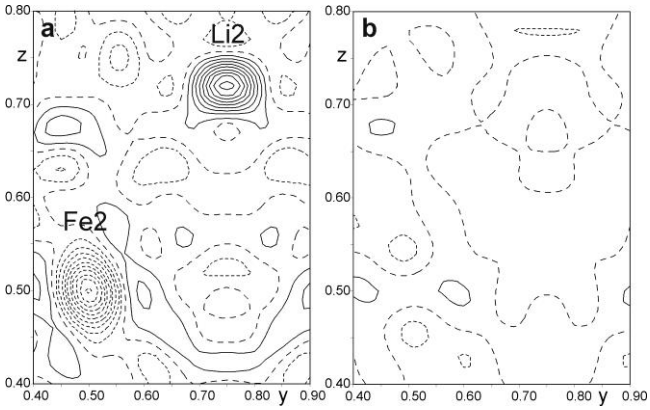

Figure 1. Difference Fourier map of the scattering density around the Li2 and Fe2 positions in the Li_2FePO_4F-75 structure refined with a complete Li/Fe ordering (a) and with antisite Li/Fe disorder (b). Solid and dashed lines correspond to positive and negative values, respectively. The contour intervals are identical on both figures.

EDX analysis of the Li_2FePO_4F-RT sample revealed a small remaining Na content corresponding to the $Li_{1.84}Na_{0.16}FePO_4F$ composition (Fig.S4). The Na atoms were placed in their native Li1 position in the refinement. The Li/Fe mixing in Li_2FePO_4F-RT was also substantial (Tables S4, S5), thus reflecting that the elevated temperature is not the primary reason for the antisite disorder. We also used the same experimental setup to cycle the olivine-structured $LiFePO_4$ at the temperature of 100 °C, as in this material the antisite defects have the lowest energy among all intrinsic defects. However, the structure refinement of the cycled $LiFePO_4$-100 sample demonstrates a complete ordering of the Li and Fe cations (Tables S6, S7). This comparison indicates that the different tendency of these two materials to the antisite disorder is most probably related to fine peculiarities of their structural organization.

One may assume that the antisite disorder was already present in the initial $LiNaFePO_4F$ compound, or that it is directly linked to the Li for Na replacement. To verify these conjectures, we prepared the $Li_xNa_{2-x}FePO_4F$ (x = 1.13, 1.68) solid solutions by chemical exchange of Li for Na using LiBr in acetonitrile at room temperature. The crystal structures of the initial material and the solid solutions were studied with synchrotron powder X-ray diffraction (Tables S8-S14, Fig. S6-S8). In none of the cases the antisite disorder was found being in agreement with the previous structural studies on the parent $LiNaFePO_4F$ and chemically prepared $Li_xNa_{2-x}FePO_4F$ materials.[21-23] The absence of antisite disorder in the initial and chemically substituted materials points to the fact that the mixing of Li and Fe occurs upon electrochemical charge of the material. Apparently, there should be some structural features of Li_2FePO_4F, which are responsible for this unusual tendency to the antisite disorder.

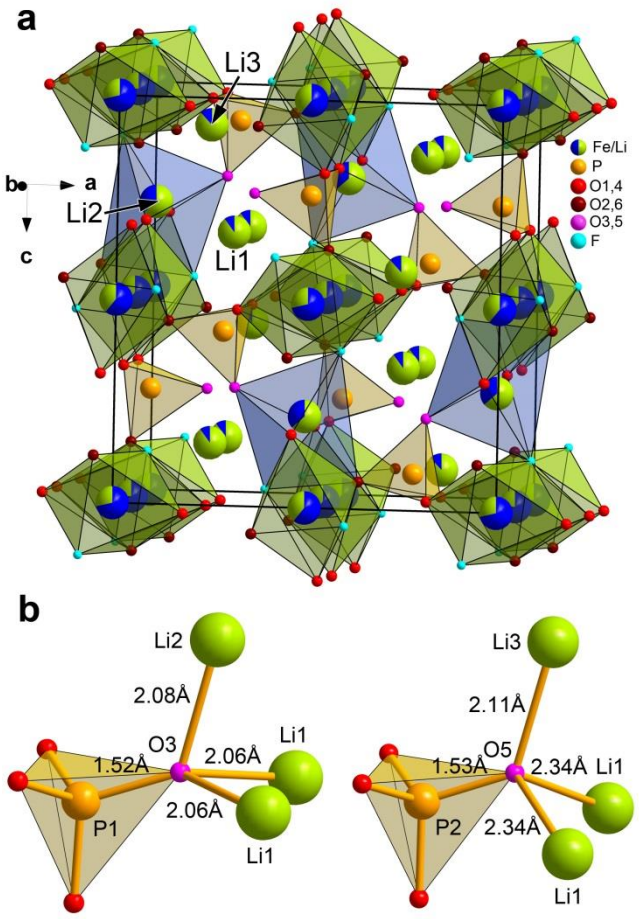

Figure 2. (a) The crystal structure of Li_2FePO_4F-75. The oxygen polyhedra around the Fe, P and Li2 positions are shown in green, orange and blue, respectively. (b) The local coordination environment of the O3 and O5 positions.

The Li_2FePO_4F-75 crystal structure is shown in Fig. 2a (see also Fig. S9). The structure consists of infinite chains of edge-sharing FeO_4F_2 octahedra running along the *b*-axis. The chains are linked into a 3-dimensional framework by PO_4 groups sharing three common oxygens with the octahedral chains. The fourth oxygen atom of the PO_4 groups (O3 and O5) is always directed toward the tunnels in the framework formed by the octahedral chains and phosphate groups and bonded to the cations in the Li positions. The edge-sharing connectivity of the FeO_4F_2 octahedra and the "dangling" P1-O3 and P2-O5 bonds with terminating oxygens forming no bonds with the Fe cations are the key features differing the Li_2FePO_4F structure from its $LiFePO_4$ counterpart. In the latter, the FeO_6 octahedra are corner-sharing and all the oxygen atoms of the PO_4 groups are bonded to Fe.

The cation coordination of the O3 and O5 atoms in Li_2FePO_4F deserves special attention. These oxygen atoms are tetrahedrally coordinated with one P and three Li cations, and two of these lithiums reside in the position Li1 (Fig. 2b). Upon charge, Li1 is the only electrochemically active position,[24,25] and in the hypothetical fully delithiated $LiFePO_4F$ material this position is empty, leaving the O3 and O5 atoms severely underbonded. Indeed, upon complete removal of the cations from the Li1 position, the BVS for the O3 and O5 positions amounts to 1.54 and 1.56, respectively. This missing bond valence cannot be compensated by the remaining P-O and Li-O bonds, unless, e.g., the P-O bond would shorten to ~1.4 Å, which is significantly shorter than the sum of the ionic radii of P^{5+} and O^{2-} (0.17Å and 1.35Å, respectively). The replacement of Li^+ with the Fe^{3+} cations of higher charge would be a plausible way to partially mitigate this bond misbalance. Adding one Fe^{3+} atom to the coordination sphere of these oxygens restores the BVS to 2.02 and 1.75, much closer to the nominal value.

Additional bond misbalance originates from the oxygen atoms O2 and O6 residing at the common edge of the FeO_4F_2 octahedra. In a fully ordered pristine structure, these atoms are already slightly overbonded (BVS of 2.16 and 2.12, respectively), whereas the replacement of Fe^{2+} with Fe^{3+} would raise their BVS even further, to 2.22 and 2.19, respectively. The O2 and O6 atoms are not bonded to the electrochemically active Li1 cations and the removal of Li upon charge will not directly affect their BVS. Breaking the infinite chain of the Fe-O-Fe bonds by introducing the Fe-O-Li fragments due to antisite disorder normalizes the BVS for the O2 and O6 atoms (2.10 and 1.98 in the Li_2FePO_4F-75 structure). Since both the "dangling" P-O bonds and edge-sharing connectivity of the FeO_6 octahedra are absent in $LiFePO_4$, these features naturally explain the higher tendency toward antisite disorder in Li_2FePO_4F compared to $LiFePO_4$.

Our qualitative analysis is confirmed by a direct *ab initio* calculation of defect energies (see Supporting information). In the delithiated $LiFePO_4F$ structure, the most stable antisite defect involves an exchange of atoms in the Li2 and Fe2 positions and has an energy of 0.29 eV, more than twice lower than 0.65–0.72 eV in $LiFePO_4$. The lowest energy of defect formation is at the Li2 site that is consistent with the largest disorder at Li2 observed experimentally. The next most stable antisite defect with the energy of 0.42 eV involves Li3 and Fe1. The most stable Li2-Fe2 defect structure indeed features a short distance of 1.91 Å between the Fe2 atom on the Li site and the O3 atom of the "dangling" bond, which then gains the missing bond valence.

$LiNaFePO_4F$ reveals a discharge capacity of ~112 mAh/g at 75 °C with ~15% capacity fade after 10 charge/discharge cycles in the 2.6 – 4.0V potential range at the C/10 rate (Fig. S1a). At the same time, LiFePO4, cycled at 100 °C within nearly the same potential range of 2.2 – 4.1V, does not show any capacity fade (Fig. S1b). This indicates that the observed Li/Fe disorder might be an obstacle to the Li diffusion partially blocking the Li positions that could lead to a capacity fade. Nevertheless, a moderate capacity fade of 15% at quite substantial antisite disorder should not be surprising, particularly in the light of good electrochemical performance of some cation-disordered systems due to a formation of percolated diffusion paths.[7,25] One should note, however, that there is some controversy in the reported capacity fade of $LiNaFePO_4F$ at room temperature: Ben Yahia *et al.* noticed a significant capacity decrease when the sample was cycled between 1.0 V and 4.4-4.5 V, or between 1.3 V and 4.8 V (C/5 rate).[21,23] Kosova *et al.* reported good capacity retention in the 2.0 – 5.0 V potential range at least for 12 cycles,[22] whereas Khasanova *et al,* demonstrated capacity drop at the C/50 rate and even a slight capacity increase from ~70 to 75 mAh/g when the material was cycled at C/10 between 2.0 and 4.5V.[18] These controversial data do not allow us to establish an unequivocal relation between the capacity fade and antisite Li/Fe disorder, although this relationship is likely to exist. A more de-

tailed analysis on a series of samples measured under the same conditions and characterized by structure refinement may shed light on the impact of the antisite disorder on the capacity fade.

Altogether, in Li_2FePO_4F the presence of the oxygen atoms linked exclusively to Li and P atoms ("dangling" P-O bonds) results in a substantial bond misbalance when Li is deintercalated upon electrochemical charging. The missing bond valence is re-stored through Fe migration toward the Li positions, which triggers the Li/Fe antisite disorder. The edge-sharing connectivity of the FeO_4F_2 octahedra may also promote the antisite disorder, because oxygen atoms at the common edge of the two octahedra form no bonds with the electrochemically active Li cations. Antisite disorder relieves the overbonding of these oxygens in the charged state. The "dangling" A-O bonds of the polyanion AO_4 groups are not unique to the Li_2FePO_4F structure and can be also found in other cathode materials, such as layered Na_2FePO_4F, $Li_2Fe(SO_4)_2$, and $Na_4Fe_3(PO_4)_2(P_2O_7)$.[26-29] The need for bond compensation of these oxygen atoms may trigger antisite disorder upon electrochemical charge in these materials too. The occurrence, degree and reversibility of this anitisite disorder calls for a detailed investigation of these and other similar compounds in the charged, discharged and cycled states.

ASSOCIATED CONTENT

Supporting Information. Experimental details, procedures of the EDT and Rietveld structure refinement, structural and bonding parameters, electron diffraction data, electrochemistry data, EDX spectra, crystallographic information. This material is available free of charge via the Internet at http://pubs.acs.org.

AUTHOR INFORMATION

Corresponding Author

* E-mail: a.abakumov@skoltech.ru

Author Contributions

The manuscript was written through contributions of all authors. All authors have given approval to the final version of the manuscript.

ACKNOWLEDGMENT

The work was supported by Russian Science Foundation (grant 16-19-00190). J. Hadermann, O. M. Karakulina, and A. M. Abakumov acknowledge support from FWO under grant G040116N.

REFERENCES

(1) Sathiya, M.; Abakumov, A. M.; Foix, D.; Rousse, G.; Ramesha, K.; Saubanère, M.; Doublet, M. L.; Vezin, H.; Laisa, C. P.; Prakash, A. S.; Gonbeau, D.; VanTendeloo, G.; Tarascon, J-M. Origin of voltage decay in high-capacity layered oxide electrodes. *Nature Mater.* **2015** 14, 230–238.

(2) Abdellahi, A.; Urban, A.; Dacek, S.; Ceder, G. Understanding the Effect of Cation Disorder on the Voltage Profile of Lithium Transition-Metal Oxides. *Chem. Mater.* **2016**, Article ASAP, DOI: 10.1021/acs.chemmater.6b01438.

(3) Choi, S.; Manthiram, A. Factors Influencing the Layered to Spinel-like Phase Transition in Layered Oxide Cathodes. *J. Electrochem. Soc.* **2002** 149, A1157-A1163.

(4) Mohanty, D.; Sefat, A. S.; Kalnaus, S.; Li, J.; Meisner, R. A.; Payzant, E. A.; Abraham, D. P.; Wood, D. L.; Daniel, C. Investigating phase transformation in the $Li_{1.2}Co_{0.1}Mn_{0.55}Ni_{0.15}O_2$ lithium-ion battery cathode during high-voltage hold (4.5 V) *via* magnetic, X-ray diffraction and electron microscopy studies. *J. Mater. Chem. A* **2013** 1, 6249–6261.

(5) Xu, B.; Fell, C. R.; Chi, M.; Meng, Y. S. Identifying surface structural changes in layered Li-excess nickel manganese oxides in high voltage lithium ion batteries: A joint experimental and theoretical study. *Energy Environ. Sci.* **2011** 4, 2223-2233.

(6) Ito, A.; Shoda, K.; Sato, Y.; Hatano, M.; Horie, H.; Ohsawa, Y. Direct observation of the partial formation of a framework structure for Li-rich layered cathode material $Li[Ni_{0.17}Li_{0.2}Co_{0.07}Mn_{0.56}]O_2$ upon the first charge and discharge. *J.Power Sources* **2011** 196, 4785–4790.

(7) Genevois, C.; Koga, H.; Croguennec, L.; Ménétrier, M.; Delmas, C.; Weill, F. Insight into the Atomic Structure of Cycled Lithium-Rich Layered Oxide $Li_{1.20}Mn_{0.54}Co_{0.13}Ni_{0.13}O_2$ Using HAADF STEM and Electron Nanodiffraction. *J. Phys. Chem. C* **2015** 119, 75–83.

(8) Lee, J.; Urban, A.; Li, X.; Su, D.; Hautier, G.; Ceder, G. Unlocking the Potential of Cation-Disordered Oxides for Rechargeable Lithium Batteries. *Science* **2014** 343, 519-522.

(9) Croguennec, L.; Palacin, M. R. Recent Achievements on Inorganic Electrode Materials for Lithium-Ion Batteries. *J. Am. Chem. Soc.* **2015** 137, 3140–3156.

(10) Ellis, B. L.; Lee, K. T.; Nazar, L. F. Positive Electrode Materials for Li-Ion and Li-Batteries. *Chem. Mater.* **2010**, 22, 691–714.

(11) Shannon, R. D. Revised effective ionic radii and systematic studies of interatomic distances in halides and chalcogenides. *Acta Cryst.* **1976** A32, 751-767.

(12) Islam, M. S.; Driscoll, D. J.; Fisher, C. A. J.; Slater, P. R. Atomic-Scale Investigation of Defects, Dopants, and Lithium Transport in the $LiFePO_4$ Olivine-Type Battery Material. *Chem. Mater.* **2005** 17, 5085-5092.

(13) Chen, J.; Graetz, J. Study of Antisite Defects in Hydrothermally Prepared $LiFePO_4$ by in Situ X-ray Diffraction. *ACS Appl. Mater. Interfaces* **2011** 3, 1380–1384.

(14) Jensen, K.; Christensen, M.; Tyrsted, C.; Brummerstedt Iversen, B. Real-time synchrotron powder X-ray diffraction study of the antisite defect formation during sub- and supercritical synthesis of $LiFePO_4$ and $LiFe_{1-x}Mn_xPO_4$ nanoparticles. *J. Appl. Cryst.* **2011** 44, 287–294.

(15) Hu, B.; Tao, G. Molecular dynamics simulations on lithium diffusion in $LiFePO_4$: the effect of anti-site defects. *J. Mater. Chem. A* **2015** 3, 20399-20407.

(16) Boulineau, A.; Gutel, T. Revealing Electrochemically Induced Antisite Defects in $LiCoPO_4$: Evolution upon Cycling. *Chem. Mater.* **2015** 27, 802–807.

(17) Khasanova, N. R.; Drozhzhin, O. A.; Storozhilova, D. A.; Delmas, C.; Antipov, E. V. New form of Li_2FePO_4F as cathode material for Li-ion batteries. *Chem. Mater.* **2012** 24, 4271–4273.

(18) Antipov, E. V.; Khasanova, N. R.; Fedotov, S. S. Perspectives on Li and transition metal fluoride phosphates as cathode materials for a new generation of Li-ion batteries *IUCrJ* **2015** 2, 85–94.

(19) Drozhzhin, O. A.; Sumanov, V. D.; Karakulina, O. M.; Abakumov, A. M.; Hadermann, J.; Baranov, A. N.; Stevenson, K. J.; Antipov, E. V. Switching between solid solution and two-phase regimes in the $Li_{1-x}Fe_{1-y}Mn_yPO_4$ cathode materials during lithium (de)insertion: combined PITT, in situ XRPD and electron diffraction tomography study. *Electrochimica Acta* **2016** 191, 149–157.

(20) Fedotov, S. S.; Khasanova, N. R.; Samarin, A. Sh.; Drozhzhin, O. A.; Batuk, D.; Karakulina, O. M.; Hadermann, J.; Abakumov, A. M.; Antipov, E. V. $AVPO_4F$ (A = Li, K): A 4 V Cathode Material for High-Power Rechargeable Batteries *Chem. Mater.* **2016** 28, 411–415.

(21) Ben Yahia, H.; Shikano, M.; Sakaebe, H.; Koike, S.; Tabuchi, M.; Kobayashi, H.; Kawaji, H.; Avdeev, M.; Miiller, W.; Ling, C. D. Synthesis and characterization of the crystal structure, the magnetic and the electrochemical properties of the new fluorophosphate $LiNaFe[PO_4]F$. *Dalton Trans.* **2012** 41, 11692–11699.

(22) Kosova, N. V.; Podugolnikov, V. R.; Bobrikov, I. A.; Balagurov, A. M. Crystal structure and electrochemistry of $Na_{2-x}Li_xFePO_4F$ ($0 \leq \times \leq 1$) new cathode materials for Na-and Li-ion batteries. *ECS Transactions* **2014** 62, 67-78.

(23) Ben Yahia, H.; Shikano, M.; Koike, S.; Sakaebe, H.; Tabuchi, M.; Kobayashi, H. New fluorophosphate $Li_{2-x}Na_xFe[PO_4]F$ as cathode material for lithium ion battery. *J. Power Sources* **2013** 244, 87–93.
(24) Khasanova, N. R.; Gavrilov, A. N.; Antipov, E. V.; Bramnik, K. G.; Hibst, H. Structural transformation of Li_2CoPO_4F upon Li-deintercalation. *J. Power Sources* **2011** 196, 355–360.
(25) Yabuuchi, N.; Takeuchi, M.; Nakayama, M.; Shiiba, H.; Ogawa, M.; Nakayama, K.; Ohta, T.; Endo, D.; Ozaki, T.; Inamasu, T.; Sato, K.; Komaba, S. High-capacity electrode materials for rechargeable lithium batteries: Li_3NbO_4-based system with cation-disordered rocksalt structure. *Proc. Nat. Acad. Sci.* **2015** 112, 7650–7655.
(26) Ellis, B. L.; Makahnouk, W. R. M.; Rowan-Weetaluktuk, W. N.; Ryan, D. H.; Nazar, L. F. Crystal Structure and Electrochemical Properties of A_2MPO_4F Fluorophosphates (A = Na, Li; M = Fe, Mn, Co, Ni). *Chem. Mater.* **2010** 22, 1059-1070.
(27) Reynaud, M.; Rousse, G.; Chotard, J.-N.; Rodriguez-Carvajal, J.; Tarascon, J.-M. Marinite $Li_2M(SO_4)_2$ (M = Co, Fe, Mn) and $Li_1Fe(SO_4)_2$: Model Compounds for Super-Super-Exchange Magnetic Interactions. *Inorg. Chem.* **2013** 52, 10456-10466.
(28) Lander, L.; Reynaud, M.; Rousse, G.; Sougrati, M. T.; Laberty-Robert, C.; Messinger, R. J.; Deschamps, M.; Tarascon, J.-M. Synthesis and Electrochemical Performance of the Orthorhombic $Li_2Fe(SO_4)_2$ Polymorph for Li-Ion Batteries. *Chem. Mater.* **2014** 26, 4178–4189.
(29) Kim, H.; Park, I.; Seo, D.-H.; Lee, S.; Kim, S.-W.; Kwon, W. J.; Park, Y.-U.; Kim, C. S.; Jeon, S.; Kang. K. New Iron-Based Mixed-Polyanion Cathodes for Lithium and Sodium Rechargeable Batteries: Combined First Principles Calculations and Experimental Study. *J. Am. Chem. Soc.* **2012** 134, 10369-10372.

Table of Contents artwork